Chemical Engineering Journal 161 (2010) 73–82

Contents lists available at ScienceDirect

Chemical Engineering Journal

journal homepage: www.elsevier.com/locate/cej

Adsorption of Co(II) and Ni(II) by EDTA- and/or DTPA-modified chitosan: Kinetic and equilibrium modeling

Eveliina Repo[a,*], Jolanta K. Warchol[c], Tonni Agustiono Kurniawan[a,1], Mika E.T. Sillanpää[a,b,1]

[a] Laboratory of Applied Environmental Chemistry (LAEC), The University of Eastern Finland, Patteristonkatu 1, FI-50100 Mikkeli, Finland
[b] Faculty of Technology, Lappeenranta University of Technology, Patteristonkatu 1, FI-50100 Mikkeli, Finland
[c] Rzeszów University of Technology, Department of Water Purification and Protection, 6 Powstanïców Warszawy Street, 35-959 Rzeszów, Poland

ARTICLE INFO

Article history:
Received 10 February 2010
Received in revised form 14 April 2010
Accepted 15 April 2010

Keywords:
Modified chitosan
Adsorption isotherm
Metal removal
EDTA
DTPA
Binary system

ABSTRACT

The aim of the present study was to investigate the adsorption properties of surface modified chitosans in the aqueous solutions containing Co(II) and/or Ni(II) ions. For this purpose, the ligands of ethylenediaminetetraacetic acid (EDTA) or diethylenetriaminepentaacetic acid (DTPA) were immobilized onto polymer matrices of chitosan. Adsorption of Co(II) and Ni(II) by prepared adsorbents was investigated in batch techniques. The effects of pH, functional group, contact time, and the concentration of metals were studied. Metal uptake by EDTA-chitosan was 63.0 mg g^{-1} for Co(II) and 71.0 mg g^{-1} for Ni(II) and by DTPA-chitosan 49.1 mg g^{-1} for Co(II) and 53.1 mg g^{-1} for Ni(II). The adsorption efficiency of studied adsorbents ranged from 93.6% to 99.5% from 100 mg L^{-1} Co(II) and/or Ni(II) solution, when the adsorbent dose was 2 g L^{-1} and solution pH 2.1. The kinetics of Co(II) and Ni(II) on both of the modified chitosans followed the pseudo-second-order model but the adsorption rate was also influenced by intraparticle diffusion. The equilibrium data was best described by the Sips isotherm and its extended form was also well fitted to the two-component data obtained for systems containing different ratios of Co(II) and Ni(II). Nevertheless, the obtained modeling results indicated relatively homogenous system for Co(II) and heterogeneous system for Ni(II) adsorption.

1. Introduction

The increasing level of toxic metals such as Co(II) and Ni(II) that are discharged into the environment as industrial wastes, represent a serious threat to human health, living resources, and ecological systems [1]. Co(II) is present in the wastewater of nuclear power plants and many other industries such as mining, metallurgical, electroplating, paints, pigments, and electro-engineering [2]. Ni(II) is widely used in silver refineries, electroplating, zinc base casting, and storage battery industries [3].

Various technologies have been applied to remove Co(II) and Ni(II) from waste streams. These include chemical precipitation [4], chemical oxidation/reduction [5], and electrochemical treatment [6]. However, all of the above methods have disadvantages making them less technically appealing in wastewater treatment. Precipitation is ineffective and produces a lot of sludge, chemical reduction/oxidation requires extra chemicals and electrochemical treatment has high operating costs [7,8].

One of the most effective methods for the removal of Co(II) and Ni(II) from wastewater streams is adsorption. Activated carbon has been the most popular material in wastewater treatment for heavy metal removal. However, the high cost of this material makes its application less economically attractive in industrial scale [9]. Cation-exchange resins used for Co(II) and Ni(II) removal can produce treated effluents that contain metals less than the required discharge limits [10]. However, commercial resins remain expensive materials [7]. To reduce the operational costs, the search for alternative adsorbents has intensified in recent years. For example, natural bentonite [2], orange peel [11], chitosan [12–15], and anaerobic granular sludges [16,17] have been tested for heavy metal removal. However, these materials have usually low adsorption capacities in as-received forms. To improve their performance, non-conventional materials such as chitosan needs to be modified chemically.

Due to the reactivity of amine groups and stable chelation, chitosan can be functionalized to improve its adsorption properties [15]. Chemical modification of chitosan with chelating agents such as ethylenediaminetetraacetic acid (EDTA) and diethylenetriaminepentaacetic acid (DTPA), which form very strong chelates with metal ions [18,19] may produce adsorbents with excellent metal binding properties. The environmental fate of these chelating agents has received attention, but, when immobilized, EDTA and

* Corresponding author. Tel.: +358 15 355 3707; fax: +358 15 355 6363.
E-mail address: eveliina.repo@uef.fi (E. Repo).
[1] Tel.: +358 15 355 3707; fax: +358 15 355 6363.

1385-8947/$ – see front matter © 2010 Elsevier B.V. All rights reserved.
doi:10.1016/j.cej.2010.04.030

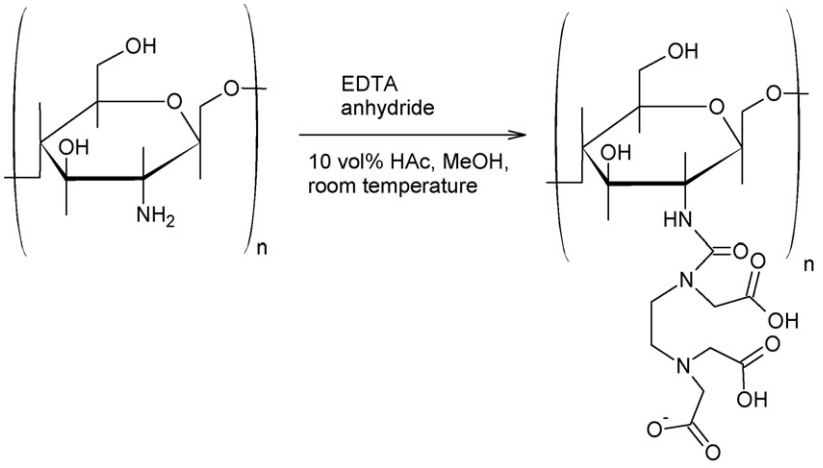

Fig. 1. Synthesis of EDTA-chitosan.

DTPA are not expected to be environmentally critical compounds [20]. Inoue et al. studied quite extensively adsorption of metals such as Cd, Fe, Cu, Ni, Co, and Zn by EDTA- and DTPA-chitosans [21,22]. However, their work lacked of simulation modeling of adsorption kinetics and isotherms of the adsorbents as well as adsorption mechanism and regeneration studies. Therefore, the aim of this study was to investigate the adsorption properties of these promising materials in more detail.

In the previous study, we investigated the applicability of EDTA- and/or DTPA-modified silica gels to remove Co(II) and Ni(II) from contaminated water at optimized conditions [23]. In this work, EDTA- and DTPA-chitosans were used to adsorb Co(II) and Ni(II) from aqueous solutions. The effects of variables including the type of chelating agent, metal concentration, and pH on the adsorption capacity, selectivity and desorption properties of the modified chitosan were considered. To investigate the mechanism of adsorption the gathered experimental data was fitted to kinetic and equilibrium models. Furthermore, equilibrium behavior of modified chitosans was investigated in Co(II)/Ni(II) two-component systems and obtained data modeled using binary isotherm selected based on the modeling results of one-component systems.

2. Methods

2.1. Materials

Chitosan flakes >85% deacetylated supplied by Sigma–Aldrich had molecular weight ranging from 190,000 to 375,000 g mol^{-1} and viscosity of 200–2000 MPa. All other chemicals used in this study were of analytical grade and supplied by Merck (Finland). Stock solutions of 1000 mg L^{-1} were prepared by dissolving appropriate amounts of Co(II) and Ni(II) nitrate salts in double deionized water. Working solutions ranging from 1 to 200 mg L^{-1} of Co(II) or Ni(II) were prepared by diluting the stock solutions. Adjustment of pH was carried out using 0.1 M NaOH and 0.1 M HNO_3.

2.2. Synthesis of EDTA- and/or DTPA-modified chitosan

To improve its reactivity, chitosan was functionalized with EDTA and/or DTPA according to Nagib et al. [22] (Fig. 1). About 10 g of chitosan was dissolved in 200 mL of 10% (v/v) acetic acid and then diluted five times with methanol. Afterwards, approximately 60 g of EDTA anhydride synthesized according to Tülü and Geckeler [24] suspended in methanol was added and the mixture was stirred vigorously for 24 h in room temperature. After filtration the precipitation was mixed with ethanol (AA) and subsequently stirred for another 16 h. Then the precipitation was washed with NaOH solution (pH 11) to remove unreacted EDTA. Finally, EDTA-modified chitosan was washed with deionized water, 0.1 M HCl, again deionized water, and ethanol. The final product was dried in an oven at 40 °C for 48 h and stored in a desiccator. Using the same method, the chitosan was functionalized with DTPA.

2.3. Characterization of modified chitosans

The formation of additional functional groups on chitosan surface after modification with EDTA and/or DTPA was studied using a FTIR-spectroscope type Nicolet Nexus 8700 (USA). Kjeldahl method was employed to determine the amount of nitrogen in the modified chitosans [25] and the results were used to determine the surface coverage of EDTA and DTPA on the adsorbents. The specific surface area and total pore volume of modified chitosans were measured with Autosorb-1-C surface area and pore size analyzer (Quantachrome, the UK).

2.4. Batch adsorption tests

Applicability of modified chitosans for Co(II) and Ni(II) removal was studied using batch experiments in a reaction mixture of 0.01 g of adsorbent and 0.005 L of metal solution containing Co^{2+} and/or Ni^2 at concentrations ranging from 1 to 200 mg L^{-1}. To study adsorption equilibrium in binary systems, solutions containing Co(II) and Ni(II) at ratios of 1:1, 2:1, and 1:2, where total concentration of metals varied from 1 to 500 mg L^{-1}, were used. The effect of pH was studied at metal concentration of 100 mg L^{-1} in the pH range of 1–7. Alkalic solutions were not used to avoid the hydroxide formation (Visual MINTEQ ver. 2.53). The effect of contact time was studied at metal concentrations of 20 and 100 mg L^{-1}. Agitation was undertaken using a rotary shaker type ST5 (CAT M.Zipperer GmbH, Staufen, Germany). At designated contact time, the adsorbent was separated from the solution using 0.45 μm polypropylene syringe filter. After dilution with 2% HNO_3, the metal concentrations in the filtrates were analyzed by an inductively coupled plasma optical atomic emission spectrometry (ICP-OES) model iCAP 6300 (Thermo Electron Corporation, USA). Co(II) was analyzed at a wavelength of 228.616 nm, while Ni(II) was detected at 231.605 nm. The detection limits for Co(II) and Ni(II) were 0.4 and 0.8 μg L^{-1}, respectively. The adsorption capacities (mg g^{-1}) of modified chitosans were calculated as follows:

$$q_e = \frac{C_i - C_e}{M} V \quad (1)$$

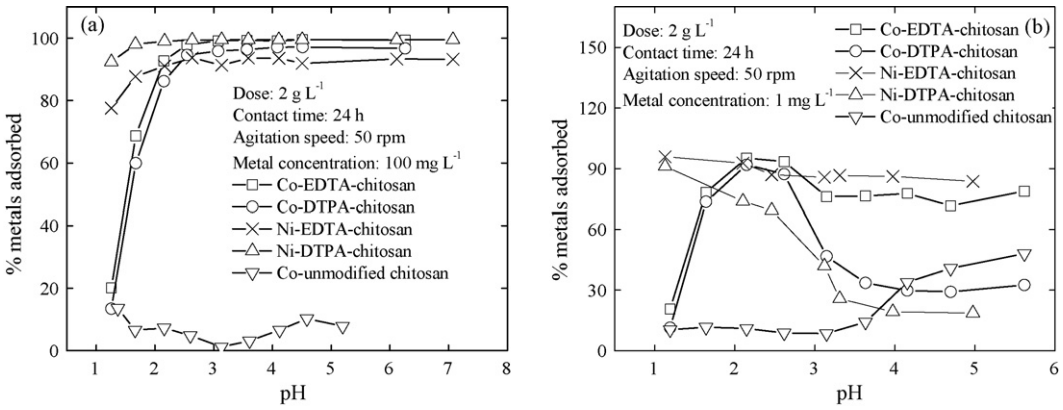

Fig. 2. Effects of pH on adsorption of Co(II) and Ni(II) by unmodified and modified chitosans.

where C_i and C_e are the initial and the equilibrium concentrations, respectively (mg L^{-1}), while M (g) and V (L) represent the weight of the adsorbent and the volume of the solution, respectively.

2.5. Regeneration studies

To evaluate their reusability, regeneration of the spent adsorbents were performed in acidic conditions. At first adsorbents were loaded by metal ions by mixing around 0.08 g of the adsorbent with 0.02 L of 100 mg L^{-1} Co(II) or Ni(II) solution. Regeneration studies were performed using higher dose to make separation procedure easier. After attaining equilibrium, the spent adsorbent was separated from the solution by centrifuge. Metal ions were eluted using 2 M HNO_3. The regeneration efficiency (%RE) of the adsorbent was calculated using Eq. (2):

$$\%\,\mathrm{RE} = \frac{q_r}{q_0} \times 100 \quad (2)$$

where q_0 and q_r are the adsorption capacities of the adsorbents (mg g^{-1}) before and after regeneration, respectively.

2.6. Statistical analysis

All the experiments were conducted in duplicate under identical conditions. The coefficient of variation was mostly less than 1%. If the variation of the metal removal by the adsorbent exceeded 5%, an identical run was undertaken and the closer data point used. To determine the margin of error, a confidence interval of 95% was calculated for each set of the samples using Origin software version 8.0 (Microcal Software, Inc.). The obtained data were then analyzed using t-test and/or ANOVA test. Differences were considered statistically significant when $p \leq 0.05$ for the analysis of variance (ANOVA) or t-tests.

3. Results and discussion

3.1. Characterization of modified chitosans

The presence of additional functional groups on the surface of modified chitosans was studied using FTIR spectroscopy. Absorption peaks of the carbonyl groups of amides and carboxylic groups were observed at 1629 and 1729 cm^{-1}, respectively [22]. Surface coverage of EDTA and DTPA was calculated based on the difference between the amount of nitrogen in unmodified (42.1 g kg^{-1}) and modified chitosans (81.2 and 82.6 g kg^{-1}) obtained from elemental analysis. Coverages were 1.4 and 0.96 mmol g^{-1} for EDTA- and DTPA-modified chitosan, respectively. These values are considerable lower than those presented by Nagib et al. [22] (around 5.9 and 1.3 mmol g^{-1} for EDTA- and DTPA-functionalized chitosan). This is probably due to the different type of chitosan used in synthesis. However, the surface concentrations obtained in this study were well correlated to the amount of metals adsorbed (see Section 3.2.2), which supports the results of elemental analysis.

The specific surface area and the total pore volume of the EDTA-chitosan were $0.71 \pm 0.09\ m^2\ g^{-1}$ and $1.76 \pm 0.09 \times 10^{-3}\ cm^3\ g^{-1}$, respectively. For DTPA-chitosan substantially lower values were obtained ($0.36 \pm 0.06\ m^2\ g^{-1}$ and $0.74 \pm 0.05 \times 10^{-3}\ cm^3\ g^{-1}$). These results suggested that DTPA formed crosslinks between the amino groups of chitosan moieties more effectively than EDTA thus reducing the surface area and the total pore volume of modified adsorbent. Furthermore, the specific surface area and the total pore volume of the unmodified chitosan were $5.9 \pm 0.1\ m^2\ g^{-1}$ and $11.8 \pm 0.1 \times 10^{-3}\ cm^3\ g^{-1}$, respectively, indicating that the surface modification reduced significantly the area and pore sizes.

3.2. Pertinent factors affecting on the removal of Co(II) and Ni(II) by modified chitosans

3.2.1. Effects of pH

In adsorption, pH affects protonation of surface groups and speciation of metal ions in the solution. Therefore, optimal pH needs to be determined to maximize the removal of target metals. Fig. 2a shows the adsorption performance of chitosan materials as a function of pH. At high initial concentration metal removal increased only when pH changed from 1 to 2.5 reaching an asymptotic value (Fig. 2a) and at low initial concentration it reached a maximum at pH around 2.1 for Co(II) and at 1.1 for Ni(II) (Fig. 2b). pH 2.1 was selected for further experiments because the adsorption at pH as low as 1.1 was not effective at high initial concentration.

It is worthwhile to consider more carefully the effect of pH at low metal concentrations because in 1 mg L^{-1} metal solution a quite significant decrease of adsorption efficiency as a function of pH was observed for DTPA-chitosan (Fig. 2b). This could be due to the speciation of DTPA. Calculations with MINEQL software (Visual MINTEQ ver. 2.53) show that the dominant forms of DTPA at pH 3 to pH 5 are H_3DTPA^{-2} and H_2DTPA^{-3}. Negatively charged carboxyl groups may interact with positively charged surface amino groups and therefore crosslink with surface before bind metal ions that are found a relatively small amount in the solution. At higher metal concentrations chelation of metals is fast and crosslinking do not occur in the same extent as at lower metal concentrations (Fig. 2a). For EDTA-chitosan crosslinking is less effective most likely due to the fact that EDTA molecule is shorter. Therefore, a drop of adsorption efficiency as a function of pH at low metal concentrations is not significant in the case of EDTA-chitosan.

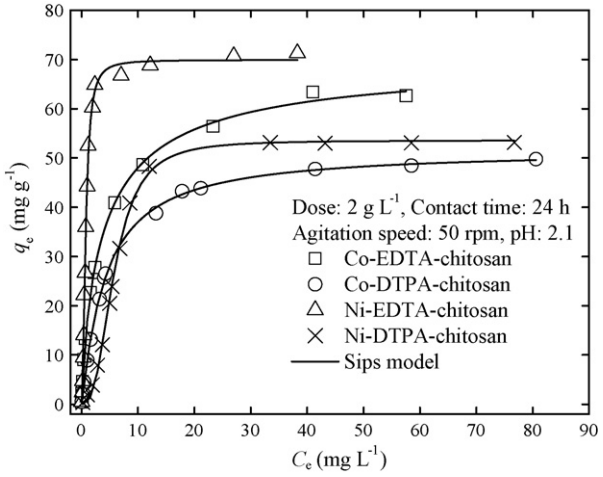

Fig. 3. Adsorption isotherms for Co(II) and Ni(II) adsorption by modified chitosans.

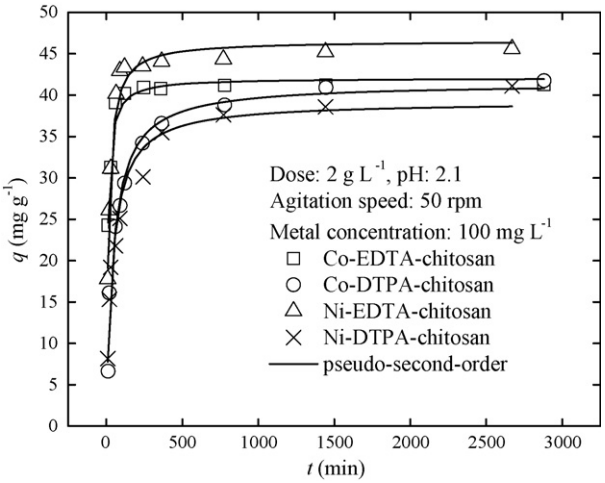

Fig. 4. Effect of contact time on Co(II) and Ni(II) adsorption by modified chitosans.

Finally, Fig. 2a shows that the removal of Ni(II) occurred at lower pH than adsorption of Co(II), which is in agreement with the earlier studies [23,26]. These results indicated that at low pH region EDTA- and DTPA-functionalized chitosans could be used for specific adsorption of Ni(II) in the presence of Co(II) (Section 3.5.3).

3.2.2. Effects of functional group

Fig. 2 shows that chemical modification of chitosan improved remarkably its adsorption performance. The removal of Co(II) by unmodified chitosan at 100 mg L^{-1} of initial concentration was only 5%, while EDTA- and DTPA-modified chitosan could almost completely remove the metal at the same operational conditions. As presented in Fig. 3, the maximum adsorption capacities of Co(II) and Ni(II) by EDTA-chitosan were 63.0 and 71.0 mg g^{-1} and by DTPA-chitosan 49.1 and 53.1 mg g^{-1}, respectively. Using the surface coverages of EDTA and DTPA, it was calculated that 72–86% of EDTA surface groups and 89–94% of DTPA surface groups were occupied by metal ions. The reason for unoccupied surface groups is most likely the crosslinking effect making some of the functionalities unable for metal binding.

In 100 mg L^{-1} metal solution the adsorption efficiency of EDTA-modified chitosan (dose: 2 g L^{-1}) was 99.2% for Co(II) and 99.5% for Ni(II). The same dose of DTPA-chitosan removed 96.7% of Co(II) and 93.6% of Ni(II) at the similar operational conditions. A higher metal removal by EDTA-chitosan could be attributed to a crosslinked structure of DTPA-chitosan (Inoue et al. [21], Section 3.1) and lower surface coverage of DTPA compared to EDTA. In addition, the higher maximum adsorption capacity of Ni(II) compared to that of Co(II) by both adsorbents was probably due to the higher stability constants of Ni(II) chelates (log K = 18.52 for EDTA and log K = 20.17 for DTPA) compared to the corresponding Co(II) chelates (log K = 16.26 for EDTA and log K = 19.15 for DTPA) [27].

In another study, Nagib et al. [22] obtained twice higher adsorption capacities for Ni(II) for both EDTA- and DTPA-functionalized chitosans. This may be due to the fact that chitosan raw materials used were different. However, the modified chitosans in this study demonstrated substantially higher adsorption capacities than similarly functionalized silica gels [23] or silica polyaminocomposites [28]. More importantly, EDTA- and DTPA-functionalized chitosans were effective adsorbents at pH ranging from 2 to 3 suggesting that they could be used in the treatment of acidic wastewater for example from electroplating industry [11].

3.2.3. Effects of contact time

The effects of contact time on the removal of Co(II) and Ni(II) by EDTA- and DTPA-modified chitosan are depicted in Fig. 4. Initially the metal uptake was fast due to the many vacant adsorption sites. For EDTA-chitosan, all the active sites were occupied by target metals within 4 h after which the adsorption rate gradually decreased and became constant at equilibrium. However, Fig. 4 shows that DTPA-chitosan needed 12 h to attain equilibrium conditions where the concentration of adsorbate in the bulk solution was in dynamic balance with that at the interface. It is possible that some of the adsorption sites of DTPA-chitosan were not as easily obtained as others due to the crosslinking (see Section 3.1). This was also seen from the slower kinetics of metal adsorption by DTPA-chitosan compared to that of EDTA-chitosan (Section 3.5.1). Due to the differences between EDTA- and DTPA-chitosans and the small increase of the adsorption capacity after 12 h of

Table 1
Regeneration of EDTA- and DTPA-chitosan for Co(II) and Ni(II) by 2 M HNO_3.

Type of adsorbent	No. of cycles	Adsorption capacity of Co(II)		Regeneration efficiency (%)	Adsorption capacity of Ni(II)		Regeneration efficiency (%)
		Before regeneration (mg g^{-1})	After regeneration (mg g^{-1})		Before regeneration (mg g^{-1})	After regeneration (mg g^{-1})	
EDTA-chitosan	1	22.96	22.66	98.73	24.35	24.34	99.99
	3	22.96	22.70	98.91	24.35	24.17	99.23
	6	22.96	22.83	99.46	24.35	24.34	99.96
	10	22.96	22.73	99.01	24.35	24.33	99.94
DTPA-chitosan	1	22.71	22.18	97.64	24.16	24.07	99.59
	3	22.71	22.49	99.02	24.16	24.10	99.73
	6	22.71	22.59	99.48	24.16	24.16	99.96
	10	22.71	22.63	99.64	24.16	24.07	99.60

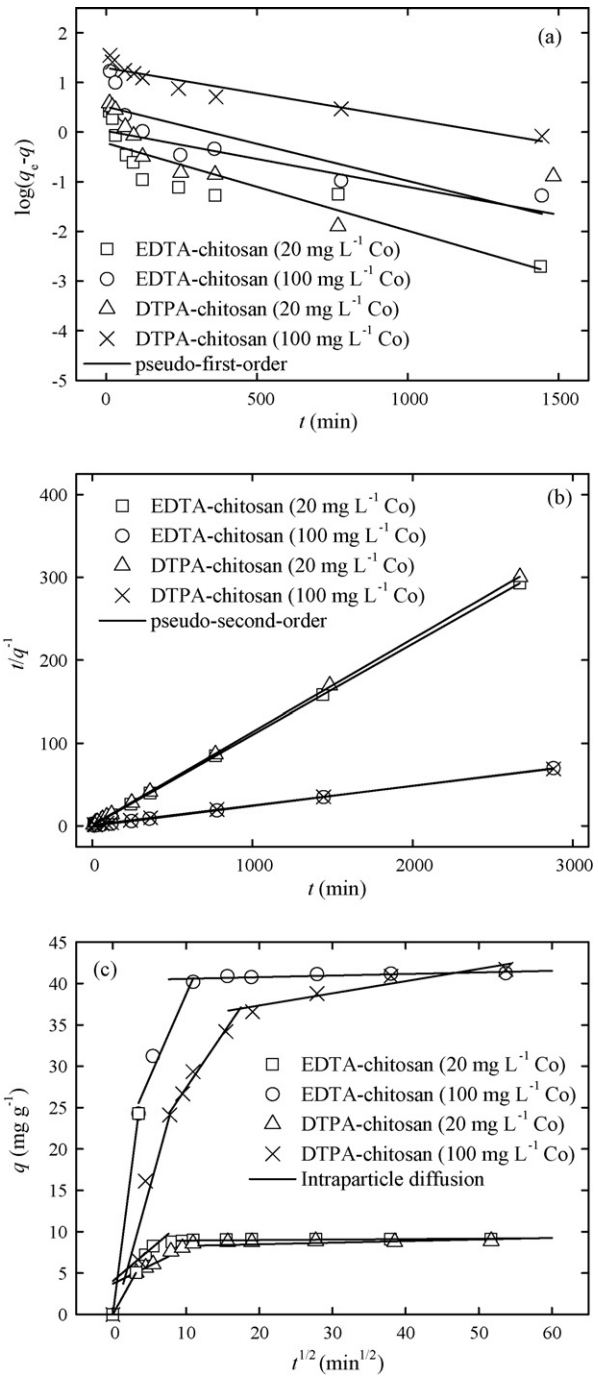

Fig. 5. Kinetic modeling of Co(II) adsorption by modified chitosans. pH: 2.1, dose: 2 g L^{-1}, and agitation speed: 50 rpm.

mixing, contact time of 24 h was selected for all the equilibrium tests.

3.3. Adsorption mechanism

On the basis of thermodynamic data [29], EDTA is represented by various species of general formula H_nEDTA^{n-4} where n ranges from 0 to 5. The calculation using the MINEQL software showed that negatively charged H_3EDTA^- (41%) and uncharged H_4EDTA (35%) were the predominant species at pH 2.1, where most of the experiments were conducted. Based on this, it is proposed that the metal removal by the modified chitosans could be presented as follows [23]:

$$RH_iEDTA^{i-3} + M^{2+} \rightleftarrows M(RHEDTA) + (i-1)H^+ \quad (3)$$

where R represents the chitosan and i is the number of hydrogen ions complexed with EDTA ranging from 2 to 3, while M^{2+} is a metal ion.

According to the above mechanism at least one proton should be released into the solution upon metal binding. However, experimentally observed amount of released protons was only half of expected against every adsorbed metal ion. This indicated that some of the protons were also bound to the surface and following protonation mechanism of free amino groups was suggested:

$$RNH_2 + H^+ \rightleftarrows RNH_3^+ \quad (4)$$

A protonation constant ($\log K_p$) of above reaction is 6.3 [30] indicating that all of the free amino groups were protonated at pH 2.1. This explains the observation that the pH did not decrease during the adsorption as much it was expected based on the reaction (3).

From the above and characterization of the modified chitosans, it was found that the chitosan surface contained some free amino groups after synthesis. Therefore, a part of the metal ions could bind on the surface also via amino groups. Earlier it has been presented that two OH groups and one amino group of chitosan are grabbed by metal ion and rest of the coordination sites are occupied by water molecules [30]:

$$RNH_2 + M^{2+} \rightleftarrows M(RNH_2)^{2+} \quad (5)$$

However, the metal binding by surface amino groups was probably highly inhibited at pH 2.1 due to the competition of protons (Eq. (4)) as could be seen in the case of unmodified chitosan (Fig. 2 [26]). Therefore, it is suggested that the metal binding occurred mainly via surface chelation by EDTA and DTPA groups. This was also supported by the similar amount of metals adsorbed vs. the amount of chelating surface groups.

3.4. Regeneration studies

Regeneration of the spent adsorbent is necessary to restore its original adsorption capacity and it enables valuable metals to be recovered from wastewater streams for reuse. In this study, Co(II) and Ni(II) were desorbed from EDTA- and DTPA-chitosans using 2 M HNO_3. Table 1 suggests that the regeneration efficiency of both adsorbents was almost complete for both metals. These results indicate the suitability of HNO_3 as the regenerant for both adsorbents. It should also be noticed that unmodified chitosan is not stable in 2 M HNO_3 [13,14]. Therefore, it seems that the modification of chitosan with EDTA and/or DTPA stabilized chitosan to resist acidic regenerant.

3.5. Simulative modeling of adsorption data

3.5.1. Modeling of adsorption kinetics

Modeling of adsorption kinetics was conducted by using the pseudo-first-order and pseudo-second-order models. These originally empirical models have been used extensively to describe the sorption kinetics. Recently, also theoretical backgrounds for these models have been studied by Azizian [31] using the classical Theory of Activated Adsorption/Desorption and Rudzinski and Plazinski [32,33] using the Statistical Rate Theory. The pseudo-first-order model is expressed as [34]:

$$\log(q_e - q_t) = \log(q_e) - \frac{k_1}{2.303}t \quad (6)$$

Table 2
Pseudo-first-order, pseudo-second-order, and intraparticle diffusion model parameters for Co(II) and Ni(II) adsorption by modified chitosans.

		EDTA-chitosan				DTPA-chitosan			
Metal	C_0 (mg L^{-1})	$q_{e,exp}$ (mg g^{-1})	q_e (mg g^{-1})	k_1 (min^{-1})	R^2	$q_{e,exp}$ (mg g^{-1})	q_e (mg g^{-1})	k_1 (min^{-1})	R^2
Pseudo-first-order									
Co(II)	20	9.12	0.61	0.0041	0.787	8.89	2.10	0.0714	0.893
	100	41.25	3.25	0.00346	0.703	41.73	14.49	0.00115	0.733
Ni(II)	20	9.48	0.69	0.00253	0.607	7.77	2.83	0.00276	0.847
	100	45.59	7.59	0.00230	0.631	42.23	19.91	0.00115	0.887

		EDTA-chitosan				DTPA-chitosan			
Metal	C_0 (mg L^{-1})	$q_{e,exp}$ (mg g^{-1})	q_e (mg g^{-1})	k_2 (g mg^{-1} min^{-1})	R^2	$q_{e,exp}$ (mg g^{-1})	q_e (mg g^{-1})	k_2 (g mg^{-1} min^{-1})	R^2
Pseudo-second-order									
Co(II)	20	9.12	9.12	0.0338	1.000	8.89	8.90	0.0125	0.999
	100	41.25	41.32	0.00459	1.000	41.73	42.37	0.00044	0.999
Ni(II)	20	9.48	9.49	0.02539	1.000	7.77	7.83	0.00390	0.999
	100	45.59	45.66	0.00171	1.000	42.23	42.37	0.00036	0.998

		EDTA-chitosan			DTPA-chitosan		
Metal	C_0 (mg L^{-1})	$k_{id,1}$ (mg g^{-1} min$^{-1/2}$)	$k_{id,2}$ (mg g^{-1} min$^{-1/2}$)	$k_{id,3}$ (mg g^{-1} min$^{-1/2}$)	$k_{id,1}$ (mg g^{-1} min$^{-1/2}$)	$k_{id,2}$ (mg g^{-1} min$^{-1/2}$)	$k_{id,3}$ (mg g^{-1} min$^{-1/2}$)
Intraparticle diffusion model							
Co(II)	20	2.043	0.751	0.0059	1.594	0.433	0.035
	100	6.933	3.438	0.019	3.196	1.105	0.147
Ni(II)	20	1.723	1.390	0.0048	0.828	0.196	0.023
	100	5.626	4.494	0.058	3.309	1.008	0.198

The pseudo-second-order rate equation is:

$$\frac{t}{q_t} = \frac{1}{k_2 q_e^2} + \frac{1}{q_e} t \tag{7}$$

where q_t and q_e (mg/g) are the adsorption capacity at time t and at equilibrium, respectively, while k_1 (min^{-1}) and k_2 (g mg^{-1} min^{-1}) are the pseudo-first-order and pseudo-second-order rate constants. Fig. 5a and Table 2 indicate that pseudo-first-order model was not representative to describe the experimental data. This could be due to the fact that pseudo-first-order model is generally applicable only at initial stage of adsorption [34,35]. However, according to Table 2, it is evident that the pseudo-second-order model (Eq. (7)) gave the best fit to the experimental data since $q_{e,exp}$ and $q_{e,model}$ were very close to each other. Thus, the main process resistance could be related to the kinetics of the sorption process [34]. Furthermore, according to the Azizian's theory [31], the sorption fits better to the pseudo-second-order model than to the first-order model when the initial concentration of the adsorbate is not excessively high, which was also the case in this study. The values of the pseudo-second-order rate constants showed faster adsorption kinetics for EDTA-chitosan compared to DTPA-chitosan.

The above theory considers kinetics governed by the rates of the surface reactions. Furthermore, to investigate if film or pore diffusion was the controlling step in the adsorption, a model of intraparticle diffusion was tested as follows:

$$q = k_{id} t^{1/2} + C \tag{8}$$

where k_{id} (mg g^{-1} min$^{-1/2}$) is the rate constant of intraparticle diffusion and C (mg g^{-1}) represents the thickness of the boundary layer. More than one linear portion in the plot of adsorption capacity vs. square root of time (Fig. 5c) indicated that the adsorption of metals by modified chitosans occurred via several steps. The first portion with steep slope represented external surface adsorption or instantaneous adsorption stage. The second portion was the gradual adsorption stage (diffusion in mesopores), where the intraparticle diffusion was rate-controlled. In the third portion (diffusion in micropores) the intraparticle diffusion started to slow down due to the low metal concentration in solution [36].

The values of intraparticle diffusion rate constants: $k_{id,1}$, $k_{id,2}$ and $k_{id,3}$ are given in Table 2. The first two rate constants were higher for EDTA-chitosan than for DTPA-chitosan indicating the faster adsorption processes for EDTA-chitosan both from the bulk phase to the exterior surface of adsorbent and inside the mesopores. The last rate constants were close to zero for EDTA-chitosan supposing the attained equilibrium state. For DTPA-chitosan no plateau was seen indicating the diffusion processes in micropores, which also seemed to be the rate controlling step [36]. Furthermore, Table 2 shows that the rate constant increased as a function of the initial concentration of metal in all three portions. This can be explained by the fact that the intraparticle diffusion model was developed based on the Fick's Law, which states that a rise in the concentration gradient increases the diffusion rate.

Based on the kinetic modeling it was suggested that both intraparticle diffusion and metal binding by the surface ligands affected the metal adsorption by the two adsorbents. Pore diffusion was not the only step that controlled the removal of the metals at the initial stage of the adsorption. This indicated that the external resistance to mass transfer was significant at the early stage of adsorption [37].

3.5.2. *Modeling adsorption isotherms for one-component systems*

Adsorption isotherms represent the adsorption capacity of the adsorbent as a function of adsorbate concentration in the solution at equilibrium conditions. Langmuir, Freundlich, and their combination Sips model were chosen for equilibrium calculations since they are commonly used in description of liquid–solid systems [38]. Modeling calculations were conducted using Origin software version 8.0 (Microcal Software, Inc.) by means of a nonlinear regression method based on the Levenberg–Marquardt algorithm. Isotherm parameters were determined by minimizing the Sum of the Squares of the Errors (ERRSQ) function across the concentration range studied:

$$\sum_{i=1}^{p} (q_{e,exp} - q_{e,calc})^2 \tag{9}$$

The Langmuir model assumes a monolayer adsorption on a homogenous surface where the binding sites have the same adsorp-

Table 3
Isotherm parameters and error analysis for modeling one-component systems by using the Langmuir and Freundlich models.

Model	Material	Type of metal	$q_{m,exp}$ (mg g^{-1})	q_m (mg g^{-1})	$K_{L/F}$ (L mg^{-1})	n	Chi^2	R^2
Langmuir	EDTA-chitosan	Co(II)	63.0	65.466	0.316		2.443	0.996
		Ni(II)	71.0	77.073	1.066		46.444	0.941
	DTPA-chitosan	Co(II)	49.1	52.866	0.222		0.447	0.999
		Ni(II)	53.1	64.139	0.116		37.027	0.924
Freundlich	EDTA-chitosan	Co(II)	63.0		9610.562	3.105	30.7223	0.947
		Ni(II)	71.0		1029074	3.930	219.166	0.720
	DTPA-chitosan	Co(II)	49.1		4878.553	3.180	32.997	0.911
		Ni(II)	53.1		668.906	2.617	93.637	0.808

tion affinity and no interactions between adsorbates are considered [38,39]:

$$q_e = \frac{q_m K_L C_e}{1 + K_L C_e} \tag{10}$$

where q_e (mg g^{-1}) and C_e (mg L^{-1}) are the adsorption capacity and the equilibrium concentration of the adsorbate, respectively, q_m (mg g^{-1}) is the maximum adsorption capacity of adsorbents, while K_L (L mg^{-1}) represents the energy of the adsorption. Fig. 3 shows that the Langmuir model correlated quite well with the experimental data for Co(II) adsorption but not that for Ni(II). For both adsorbents, the Langmuir model gave a better estimate of the maximum adsorption capacity for Co(II) (Table 3) without considerably affecting the quality of the fit.

The Freundlich model predicts the adsorption on a heterogeneous surface without saturation of adsorbent binding sites [38,39]:

$$q_e = K_F C_e^{1/n_F} \tag{11}$$

where K_F (mg g^{-1}) is a unit capacity coefficient and n_F is the Freundlich parameter related to the degree of system heterogeneity. The parameter n_F is usually greater than unity, and the larger it is, the more heterogeneous is the system [40]. The Freundlich model showed a poor fit to the experimental data with lower R^2 and the higher Chi^2 values (Table 3) in comparison to the Langmuir model. It can be seen from Fig. 3 that the data obtained experimentally formed L type adsorption isotherms providing a concave curve and tending to approach a constant value with increasing metal ion concentration [41]. The Freundlich model, unlike the Langmuir expression, does not show a maximum saturation as the aqueous concentration approaches infinity. Therefore, the equilibrium adsorption data for Co(II) and Ni(II) ion adsorption on modified chitosans were not represented appropriately by the Freundlich model in the concentration range studied.

The Sips model is a hybrid of the Langmuir and the Freundlich isotherms [39]:

$$q_e = \frac{q_m (K_S C_e)^{n_S}}{1 + (K_S C_e)^{n_S}} \tag{12}$$

where K_S (L mg^{-1}) is the Langmuir equilibrium constant and n_S is the Freundlich heterogeneity factor. The Sips isotherm behavior is the same as that of the Freundlich equation with exception of possessing a finite saturation limit when the concentration is sufficiently high. This isotherm is usually applicable where both the Langmuir and the Freundlich models fail [40]. Similar to the previous isotherm equations, the ERRSQ error function was employed to evaluate the fit of the Sips model to the experimental equilibrium data. Since the choice of error function can affect the derived parameters, the isotherm parameters for the Sips model were additionally determined by minimizing the Derivative of Marquardt's Percent Standard Deviation (MPSD) error [39]:

$$\sum_{i=1}^{p} \left(\frac{q_{e,exp} - q_{e,calc}}{q_{e,exp}} \right)^2 \tag{13}$$

A detailed error analysis was carried out to compare the calculation quality for both error functions (ERRSQ and MPSD). The isotherm parameters obtained, along with the standard deviation (σ), mean error, Chi^2 test, and correlation factor (R^2) are listed in Table 4. The comparison of the values obtained indicated that the application of different error functions resulted in different values of the Sips constants as well as the calculation errors. Based on the correlation factor R^2 a better approximation was achieved for ERRSQ. This presumption was partially confirmed by Chi^2 test. The estimated q_m values were very close to the experimentally obtained maximum metal uptake, with the exception of Co(II) adsorption on EDTA-chitosan. For this adsorbent, a slightly higher q_m value was estimated for Co(II) than for Ni(II) (70.59 and 69.90 mg g^{-1}, respectively), as opposite to that observed experimentally. The miniscule lower value of q_m for Ni(II) can result from the approximation to scattered data [42]. On the other hand, based on the standard deviation (σ) and mean error, it is evident that the fit of the Sips

Table 4
Isotherm parameters and error analysis for modeling one-component systems by using the Sips model.

Material	Type of metal	$q_{m,exp}$ (mg g^{-1})	Parameters q_m (mg g^{-1})	K_S (L mg^{-1})	n_S	Statistical tests σ	Mean error	Chi^2	R^2
ERRSQ									
EDTA-chitosan	Co(II)	63.0	70.585	0.250	0.825	0.827	10.652	0.545	0.999
	Ni(II)	71.0	69.899	1.360	1.985	2.236	7.540	2.821	0.991
DTPA-chitosan	Co(II)	49.1	51.625	0.236	1.08	0.544	3.082	0.122	0.999
	Ni(II)	53.1	53.557	0.173	2.701	1.016	17.664	27.194	0.998
MPSD									
EDTA-chitosan	Co(II)	63.0	62.985	0.370	0.974	0.067	5.297	1.010	0.993
	Ni(II)	71.0	71.520	1.248	1.849	0.101	6.284	3.584	0.987
DTPA-chitosan	Co(II)	49.1	53.008	0.215	1.031	0.038	2.597	0.198	0.999
	Ni(II)	53.1	61.360	0.111	1.502	0.234	17.178	13.091	0.931

equation to the experimental data was better for MPSD. The q_m of adsorbed Ni(II) was larger than that of Co(II) for both EDTA- and DTPA-chitosans. It corresponded to the adsorption order observed experimentally: Ni(II)EDTA > Co(II)EDTA > Ni(II)DTPA > Co(II)DTPA. Nevertheless, for DTPA-chitosan, MPSD function overestimated the real q_m value by 8–15%. All of the preceding remarks indicated that it was incorrect to select the proper error function by comparison of calculation errors when the estimated parameters were highly biased [43].

Further examination of the results represented in Table 4 indicated that the difference between the two error functions was not significant in the case of the estimation of two other Sips constants (K_S, n_S). The K_S indicated the higher affinity of Ni(II) and Co(II) for EDTA-chitosan than for DTPA-chitosan. This is analogous to the relation obtained by other authors [22]. The heterogeneity factor (n_S) values were close to unity for Co(II) adsorption indicating relatively homogenous systems [38,44]. In such a case, the Sips model reduced to the Langmuir that represented a similar extent of fit (Fig. 6a). In the case for Ni(II) adsorption, the Sips equation gave much better approximation of the experimental data, compared to both the Langmuir and the Freundlich models (Fig. 6b). The parameter n_S was greater than unity for Ni(II) adsorption, indicating system heterogeneity.

For both EDTA- and DTPA-chitosan, the heterogeneity factor n_S was higher for Ni(II) than for Co(II). It can be attributed to the structures of the chelates on the surface. The ratio of $CoHEDTA^-$ and CoH_2EDTA chelate is 1.7:1 and the ratio of $NiHEDTA^-$ and NiH_2EDTA chelate is 10.7:1 (MINEQL) at pH 2.1. The speciation in the solution phase indicates that when Ni(II) was bound on the EDTA surface group in 1:1 stoichiometry around 90% of the formed chelates had one unbound negatively charged carboxyl group. This group could have interacted with the surface or participated in binding of another Ni(II) ion. For example, two EDTA groups located close to each other could have bound altogether three Ni(II) ions and in turn increased the heterogeneity factor. In relation to DTPA there is little difference in speciation of Co(II)DTPA and Ni(II)DTPA chelates at pH 2.1. However, unbound carboxyl groups of metal DTPA chelates could have participated in binding other Ni(II) ions rather than Co(II) due to the better overall stability established for Ni(II) carboxylates compared to Co(II) carboxylates [29]. It can be concluded that the surfaces of modified chitosans had adsorption sites that were able to bind Ni(II) but not Co(II) ions.

3.5.3. Modeling adsorption isotherms for two-component systems

From the one-component systems, it was seen that the adsorption capacity of Ni(II) on both modified chitosans was higher than that of Co(II). Same characteristics were seen from adsorption tests in binary systems, where the ratio of initial concentrations of Co(II) and Ni(II) was kept constant (Co:Ni ratio: 1:1, 1:2 and 2:1). The maximum adsorption capacity of Ni(II) was two to five times higher than that of Co(II) in all the studied systems. The selectivity coefficient [45] for Ni(II), which was calculated from the ratio of the distribution constant ($q_{e,Ni}/C_{e,Ni}$) for Ni(II) over the distribution constant for Co(II) ($q_{e,Co}/C_{e,Co}$), varied for EDTA-chitosan from 56 to 102 and for DTPA-chitosan from 37 to 129. Very high values further confirmed that the modified chitosans had better selectivity and affinity for Ni(II) than for Co(II).

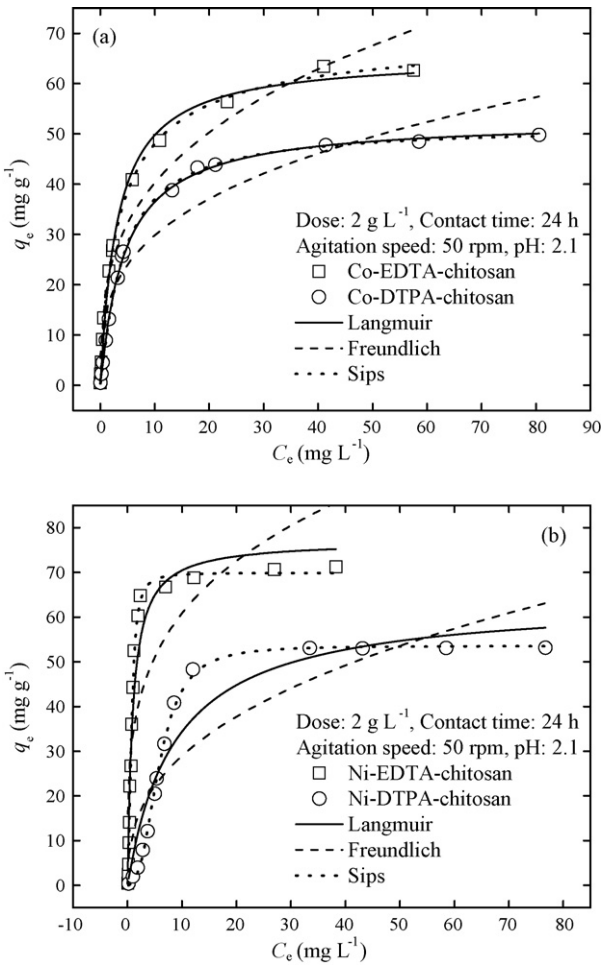

Fig. 6. Modeling of (a) Co(II) and (b) Ni(II) adsorption behavior of EDTA- and DTPA-Langmuir, Freundlich, and Sips equation.

The equilibrium data of two-component systems was modeled by usage of the extended form of the Sips isotherm [46,47]:

$$q_1 = \frac{q_{m1}(K_{S1}C_{e1})^{n_{S1}}}{1 + (K_{S1}C_{e1})^{n_{S1}} + (K_{S2}C_{e2})^{n_{S2}}} \quad (14)$$

$$q_2 = \frac{q_{m2}(K_{S2}C_{e2})^{n_{S2}}}{1 + (K_{S1}C_{e1})^{n_{S1}} + (K_{S2}C_{e2})^{n_{S2}}} \quad (15)$$

where K_{S1} and K_{S2} ($L\,mg^{-1}$) are analogous to the Langmuir affinity constants and n_{S1} are n_{S2} are heterogeneity constants. Subscriptions 1 and 2 refer to Co(II) and Ni(II), respectively. The most desirable approach to model multi-component systems is an estimation of competitive isotherm solely on the basis of the corresponding one-component isotherms [46]. However, the individual adsorption constants may not define interactions between com-

Table 5
Isotherm parameters for modeling two-component systems by using the Sips model.

Material	Parameters						Statistical tests			
	q_{m1} ($mg\,g^{-1}$)	q_{m2} ($mg\,g^{-1}$)	K_{S1} ($L\,mg^{-1}$)	K_{S2} ($L\,mg^{-1}$)	n_{S1}	n_{S2}	σ	Mean error	Chi^2	R^2
ERRSQ, q_m and n_S estimated										
EDTA-chitosan	59.852	75.012	0.250[a]	1.360[a]	0.563	1.582	36.569	74.703	30.392	0.940
DTPA-chitosan	47.983	57.075	0.236[a]	0.173[a]	0.605	3.119	23.311	79.896	19.639	0.941

Subscripts 1 and 2 refer Co(II) and Ni(II), respectively.
[a] Values taken from the one-component systems.

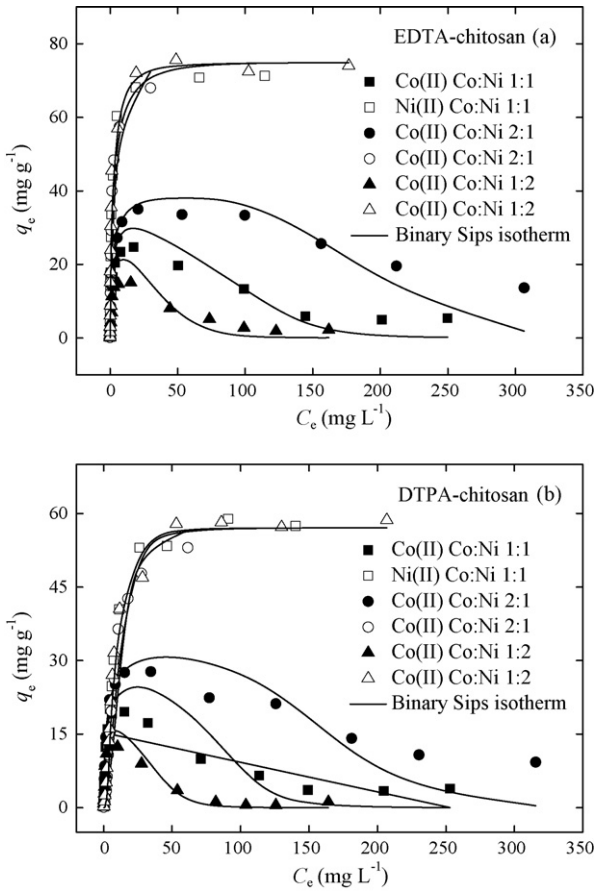

Fig. 7. Modeling of two-component data of (a) EDTA- and (b) DTPA-chitosan using the binary Sips equation. Experimental conditions as in Fig. 6.

petitive ions. The maximum adsorption capacity (q_m) as well as the interaction term (n_S) depend on the concentrations of the other components in the mixture [48]. Thus, in this part of modeling study both parameters were estimated by minimizing the ERRSQ error function (Eq. (9)). The obtained results are depicted in Table 5 and Fig. 7.

Fig. 7 shows that the binary Sips model was fitted reasonable well to the experimental two-component data. Interestingly, estimated q_m values for Ni(II) for both adsorbents were higher than those obtained for one-component systems (Tables 4 and 5). This was seen also experimentally ($q_{m,Ni(II)}$ for EDTA-chitosan 75.6 mg g^{-1} and for DTPA-chitosan 58.9 mg g^{-1} in 1:1 Co:Ni system) and indicated that the presence of Co(II) enhanced the adsorption of Ni(II). Despite of the apparent good fit, statistical tests gave quite high error values (Table 5). Especially high errors were found for low q_e values. Poorer fitting compared to the one-component systems could resulted from the K_S values applied directly from the one-component systems. Thus, it was possible that also K_S's were affected by the presence of competitive ions. On the other hand, it was reasonable to use the same K_S in one- and two-component systems due to the binding groups on the surface were chelating agents having a certain stability constant with each of the metal ions [27]. On the whole, the apparent fit, good R^2 values, and reasonable estimated q_m values supported the applicability of the Sips model also in binary systems.

4. Conclusions

EDTA- and DTPA-modified chitosans were found to effectively adsorb Co(II) and Ni(II) from aqueous solutions. The maximum metal uptake by the EDTA-chitosan was higher (q_m = 63.0 mg g^{-1} for Co(II) and q_m = 71.0 mg g^{-1} for Ni(II)) than that by the DTPA-chitosan (q_m = 49.1 mg g^{-1} for Co(II) and q_m = 53.1 mg g^{-1} for Ni(II)). At metal concentration of 100 mg L^{-1}, the removal of Co(II) and Ni(II) by the modified chitosans ranged from 93.6% to 99.5%. The selectivity sequence of both ions uptake Ni(II)EDTA/DTPA > Co(II)EDTA/DTPA was in accordance with the stability constants of the metal chelates of EDTA and DTPA. Lower metal uptake by DTPA-chitosan was attributed to its crosslinked structure and lower surface coverage of chelating groups. Adsorption kinetics followed a pseudo-second-order model for both modified chitosans, but the rate of the adsorption was also affected by intraparticle diffusion. Modeling of adsorption equilibrium required not only the choice of isotherm equation but also the error function. The quality of the fit was judged by a few statistical tests as well as accurate approximation of the real adsorption capacity (q_m). The Sips isotherm allowed the best approximation of experimental data. Nevertheless, Ni(II) and Co(II) adsorption by modified chitosan occurred under different system behavior. The adsorption studies in two-component systems showed that the modified chitosans had much better affinity for Ni(II) than for Co(II) suggesting that Ni(II) could be adsorbed selectively from the contaminated water in the presence of Co(II). Finally, the two-component equilibrium data was well described by the binary Sips model, which supported further the modeling results obtained for one-component systems.

Acknowledgements

Authors are grateful to the European Commission (Brussels) for the Marie Curie Research Fellowship for Transfer of Knowledge (No. MTKD-CT-2006-042637) and Finnish Funding Agency for Technology and Innovation (TEKES) for financial support.

References

[1] X. Huang, M. Sillanpää, B. Duo, E.T. Gjessing, Water quality in the Tibetan Plateau: metal contents of four selected rivers, Environ. Pollut. 156 (2008) 270–277.
[2] D.M. Manohar, B.F. Noeline, T.S. Anirudhan, Adsorption performance of Al-pillared bentonite clay for the removal of cobalt(II) from aqueous phase, Appl. Clay Sci. 31 (2006) 194–206.
[3] K. Kadirvelu, K. Thamaraiselvi, C. Namasivayam, Adsorption of nickel(II) from aqueous solution onto activated carbon prepared from coirpith, Sep. Purif. Technol. 24 (2001) 497–505.
[4] S.L. McAnally, T. Benefield, R.B. Reed, Nickel removal from a synthetic nickel plating wastewater using sulphide and carbonate for precipitation and coprecipitation, Sep. Sci. Technol. 19 (1984) 191–217.
[5] J. Lu, D.B. Dreisinger, W.C. Cooper, Cobalt precipitation by reduction with sodium borohydride, Hydrometallurgy 45 (1997) 305–322.
[6] K.N. Njau, M.vd. Woude, G.J. Visser, L.J.J. Janssen, Electrochemical removal of nickel ions from industrial wastewater, Chem. Eng. J. 79 (2000) 187–195.
[7] B. Volesky, Detoxification of metal-bearing effluents: biosorption for the next century, Hydrometallurgy 59 (2001) 203–216.
[8] T.A. Kurniawan, G.Y. S. Chan, W.-H. Lo, S. Babel, Physico-chemical treatment techniques for wastewater laden with heavy metals, Chem. Eng. J. 118 (2006) 83–98.
[9] S. Babel, T.A. Kurniawan, Low-cost adsorbents for heavy metals uptake from contaminated water: a review, J. Hazard. Mater. 97 (2003) 219–243.
[10] S. Rengaraj, K.-H. Yeon, S.-Y. Kang, J.-U. Lee, K.-W. Kim, S.-H. Moon, Studies on adsorptive removal of Co(II), Cr(III) and Ni(II) by IRN77 cation-exchange resin, J. Hazard. Mater. 92 (2002) 185–198.
[11] M. Ajmal, R.A.K. Rao, R. Ahmad, J. Ahmad, Adsorption studies on *Citrus reticulata* (fruit peel of orange): removal and recovery of Ni(II) from electroplating wastewater, J. Hazard. Mater. 79 (2000) 117–131.
[12] A. Bhatnagar, M. Sillanpää, Applications of chitin- and chitosan-derivatives for the detoxification of water and wastewater—a short review, Adv. Colloid Interface Sci. 152 (2009) 26–38.
[13] E. Guibal, Interactions of metal ions with chitosan-based sorbents: a review, Sep. Purif. Technol. 38 (2004) 43–74.
[14] M.N.V. Ravi Kumar, A review of chitin and chitosan applications, React. Funct. Polym. 46 (2000) 1–27.
[15] A.J. Varma, S.V. Deshpande, J.F. Kennedy, Metal complexation by chitosan and its derivatives: a review, Carbohydr. Polym. 55 (2004) 77–93.

[16] E.D. van Hullebusch, A. Peerbolte, M.H. Zandvoort, P.N.L. Lens, Sorption of cobalt and nickel on anaerobic granular sludges: isotherms and sequential extraction, Chemosphere 58 (2005) 493–505.
[17] J. Virkutyte, E. Hullebusch, M. Sillanpää, P. Lens, Copper and trace element fractionation in electrokinetically treated anaerobic granular sludge, Environ. Pollut. 138 (2005) 518–529.
[18] J. Rämö, M. Sillanpää, V. Vickackaite, M. Orama, L. Niinistö, Chelating ability and solubility of DTPA, EDTA and β-ADA in alkaline hydrogen peroxide environment, J. Pulp Paper Sci. 26 (2000) 125–131.
[19] M. Sillanpää, M. Orama, J. Rämö, A. Oikari, The importance of ligand speciation in environmental research: a case study, Sci. Total Environ. 267 (2001) 23–31.
[20] K. Pirkanniemi, S. Metsärinne, M. Sillanpää, Degradation of EDTA and novel complexing agents in pulp and paper mill process and waste waters by Fenton's reagent, J. Hazard. Mater. 147 (2007) 556–561.
[21] K. Inoue, K. Ohto, K. Yoshizuka, T. Yamaguchi, T. Tanaka, Adsorption of lead(II) ion on complexane types of chemically modified chitosan, Bull. Chem. Soc. Jpn. 70 (1997) 2443–2447.
[22] S. Nagib, K. Inoue, T. Yamaguchi, T. Tamaru, Recovery of Ni from a large excess of Al generated from spent hydrodesulfurization catalyst using picolylamine type chelating resin and complexane types of chemically modified chitosan, Hydrometallurgy 51 (1999) 73–85.
[23] E. Repo, T.A. Kurniawan, J.K. Warchol, M.E.T. Sillanpää, Removal of Co(II) and Ni(II) ions from contaminated water using silica gel functionalized with EDTA and/or DTPA as chelating agents, J. Hazard. Mater. 171 (2009) 1071–1080.
[24] M. Tülü, K.E. Geckeler, Synthesis and properties of hydrophilic polymers. Part 7. Preparation, characterization and metal complexation of carboxy-functional polyesters based on poly(ethylene glycol), Polym. Int. 48 (1999) 909–914.
[25] Standard Methods for the Examination of Water and Wastewater, 21st ed., American Public Health Association, Washington, DC, USA, 2005.
[26] K. Inoue, K. Yoshizuka, K. Ohto, Adsorptive separation of some metal ions by complexing agent types of chemically modified chitosan, Anal. Chim. Acta 388 (1999) 209–218.
[27] A.E. Martell, R.M. Smith, Critical Stability Constants, vol. 1. Amino Acids, Plenum Press, New York, 1974.
[28] M. Hughes, E. Rosenberg, Characterization and applications of poly-acetate modified silica polyamine composites, Sep. Sci. Technol. 42 (2007) 261–283.
[29] A.E. Martell, R.M. Smith, R.J. Motekaitis, NIST Critically Selected Stability Constants of Metal Complexes Database Version 3.0, Texas A&M, Texas, 1997.
[30] R.-S. Juang, F.-C. Wu, R.-L. Tseng, Adsorption removal of copper(II) using chitosan from simulated rinse solutions containing chelating agents, Water Res. 33 (1999) 2403–2409.
[31] S. Azizian, Kinetic models of sorption: a theoretical analysis, J. Colloid Interface Sci. 276 (2004) 47–52.
[32] W. Rudzinski, W. Plazinski, Kinetics of solute adsorption at solid/solution interfaces: a theoretical development of the empirical pseudo-first and pseudo-second order kinetic rate equations, based on applying the statistical rate theory of interfacial transport, J. Phys. Chem. B 110 (2006) 16514–16525.
[33] W. Rudzinski, W. Plazinski, On the applicability of the pseudo-second order equation to represent the kinetics of adsorption at solid/solution interfaces: a theoretical analysis based on the statistical rate theory, Adsorption 15 (2009) 181–192.
[34] M.S. Chiou, H.Y. Li, Adsorption behavior of reactive dye in aqueous solution on chemical cross-linked chitosan beads, Chemosphere 50 (2003) 1095–1105.
[35] G. McKay, Y.S. Ho, The sorption of lead ions on peat, Water Res. 33 (1999) 578–584.
[36] W.H. Cheung, Y.S. Szeto, G. McKay, Intraparticle diffusion processes during acid dye adsorption onto chitosan, Bioresour. Technol. 98 (2007) 2897–2904.
[37] G. McKay, M.S. Otterburn, J.A. Aga, Intraparticle diffusion process occurring during adsorption of dyestuffs, Water Air Soil Pollut. 36 (1987) 381–390.
[38] D.G. Kinniburgh, General purpose adsorption isotherms, Environ. Sci. Technol. 20 (1986) 895–904.
[39] Y.S. Ho, J.F. Porter, G. Mckay, Equilibrium isotherm studies for the sorption of divalent metal ions onto peat: copper, nickel and lead. Single component systems, Water Air Soil Pollut. 141 (2002) 1–33.
[40] D.D. Do, Adsorption Analysis: Equilibria and Kinetics, Imperial College Press, London, 1998.
[41] G. Limousin, J.-P. Gaudet, L. Charlet, S. Szenknect, V. Barthès, M. Krimissa, Sorption isotherms: a review on physical bases, modeling and measurement, Appl. Geochem. 22 (2007) 249–275.
[42] G.R. Parker, Optimum isotherm equation and thermodynamic interpretation for aqueous 1,1,2-trichloroethene adsorption isotherms on three adsorbents, Adsorption 1 (1995) 113–132.
[43] M. Chutkowski, R. Petrus, J. Warchoł, P. Koszelnik, Sorption equilibrium in processes of metal ion removal from aqueous environment. Statistical verification of mathematical models, Przem. Chem. 87 (2008) 436–438.
[44] S.K. Papageorgiou, F.K. Katsaros, E.P. Kouvelos, N.K. Kanellopoulos, Prediction of binary adsorption isotherms of Cu^{2+}, Cd^{2+} and Pb^{2+} on calcium alginate beads from single adsorption data, J. Hazard. Mater. 162 (2009) 1347–1354.
[45] H.L. Vasconcelos, E. Guibal, R. Laus, L. Vitali, V.T. Fávere, Competitive adsorption of Cu(II) and Cd(II) ions on spray-dried chitosan loaded with Reactive Orange 16, Mater. Sci. Eng. C 29 (2009) 613–618.
[46] S. Al-Asheh, F. Banat, R. Al-Omari, Z. Duvnjak, Predictions of binary sorption isotherms for the sorption of heavy metals by pine bark using single isotherm data, Chemosphere 41 (2000) 659–665.
[47] D. Kumar, A. Singh, J.P. Gaur, Mono-component versus binary isotherm models for Cu(II) and Pb(II) sorption form binary metal solution by the green alga *Pithophora oedogoni*, Bioresour. Technol. 99 (2008) 8280–8287.
[48] R.S. Vieira, E. Guibal, E.A. Silva, M.M. Beppu, Adsorption and desorption of binary mixtures of copper and mercury ions on natural and crosslinked chitosan membranes, Adsorption 13 (2007) 603–611.